HHS Public Access

Author manuscript

Nat Chem Biol. Author manuscript; available in PMC 2018 January 24.

Published in final edited form as:

Nat Chem Biol. 2017 September ; 13(9): 1016–1021. doi:10.1038/nchembio.2441.

Copper import in *Escherichia coli* by the yersiniabactin metallophore system

Eun-Ik Koh[1,2,3], **Anne E. Robinson**[1,2,3], **Nilantha Bandara**[4], **Buck E. Rogers**[4], and **Jeffrey P. Henderson**[1,2,3,*]

[1]Center for Women's Infectious Diseases Research, Washington University School of Medicine, St. Louis, Missouri, United States of America

[2]Division of Infectious Diseases, Washington University School of Medicine, St. Louis, Missouri, United States of America

[3]Department of Internal Medicine, Washington University School of Medicine, St. Louis, Missouri, United States of America

[4]Department of Radiation Oncology, Washington University School of Medicine, St. Louis, Missouri, United States of America

Abstract

Copper plays a dual role as nutrient and toxin during bacterial infections. While uropathogenic *Escherichia coli* (UPEC) strains can use the copper-binding metallophore yersiniabactin (Ybt) to resist copper toxicity, Ybt also converts bioavailable copper to Cu(II)-Ybt in low copper conditions. Although *E. coli* have long been considered to lack a copper import pathway, we observed Ybt-mediated copper import in UPEC using canonical Fe(III)-Ybt transport proteins. UPEC removed copper from Cu(II)-Ybt with subsequent re-export of metal-free Ybt to the extracellular space. Copper released through this process became available to an *E. coli* cuproenzyme (the amine oxidase TynA), linking this import pathway to a nutrient acquisition function. Ybt-expressing *E. coli* thus engage in nutritional passivation, a strategy of minimizing a metal ion's toxicity while preserving its nutritional availability. Copper acquisition through this process may contribute to the marked virulence defect of Ybt transport-deficient UPEC.

Keywords

uropathogenic *Escherichia coli*; siderophore; metal transport; copper

*Corresponding author: Center for Women's Infectious Diseases Research, Box 8051 Washington University School of Medicine,, 660 S. Euclid Ave., St. Louis, MO 63110, Phone: +13143627250, Fax: +13143623203, jhenderson@DOM.wustl.edu.

The authors have no conflicts of interest to declare.

Author Contributions: E.K., A.E.R. and J.P.H. conceived and designed the experiments. E.K. and A.E.R. performed the biochemical experiments and follow-up studies. A.E.R. conducted the ICP-MS analysis. E.K. and N.B. performed the ^{64}Cu radiolabeling experiments. E.K., A.E.R., N.B., B.E.R. and J.P.H. analyzed the data. E.K., A.E.R. and J.P.H. wrote the paper.

Competing Financial Interests: The authors declare no competing financial interests.

Introduction

Infected hosts control the chemical composition of different anatomical environments to limit microbial growth. Prominent among these compositional changes are metal ions, which may be withheld from microbes (termed “nutritional immunity”)or, conversely, deployed as antimicrobial agents [1–5]. Iron restriction is the prototypical nutritional immune response to which numerous microbial siderophore-mediated iron uptake systems have evolved as a countermeasure. In uropathogenic *Escherichia coli* (UPEC), the prominent virulence-associated siderophore yersiniabactin (Ybt), is often secreted along side enterobactin, the genetically conserved *E. coli* siderophore [6]. Originally described in *Yersinia pestis,* Ybt production is directed by asophisticated, multi-operon *Yersinia* High Pathogenicity Island (HPI), which encodes Ybt biosynthetic enzymes, membrane transporters, and a transcription factor (*ybtA*) [7–9]. *Yersinia* HPI genes are among the most highly upregulated UPEC genes during experimental urinary tract infections (UTIs)[10]. Direct mass spectrometric detection of urinary Ybt and serological detection of the outer membrane Ybt importer (FyuA) have further implicated roles for the *Yersinia* HPI in clinical UTIs[3,6,11].

Among HPI-encoded proteins, transport-associated outer and inner membrane proteins are required for Fe(III)-Ybt dependent growth and are expressed in a YbtA-dependent manner [8,9,12,13]. FyuA (ferric yersiniabactin uptake A, Psn in *Yersinia pestis*) is an outer membrane protein with structural and functional features that are typical of TonB-dependent outer membrane siderophore transporters [13,14]. YbtP and YbtQ are inner membrane ATP-binding cassette transporters typical of siderophore systems, though their specific transport specificities have not been conclusively demonstrated [9,12,15]. No catabolic enzymes or siderophore reductases are encoded within the *Yersinia* HPI to guide further investigation [16–19]. The precise fate of Ybt complexes following FyuA-mediated import is therefore incompletely understood.

Although its iron-scavenging function led Ybt to initially be classified as a siderophore, recent observations that Ybt binds and sequesters copper(II) outside the cell to resist copper toxicity suggest a broader metallophore mode of action [3,20]. Nevertheless, a recent study demonstrated a marked virulence defect in YbtPQ-null UPEC mutants during experimental UTI but not during *in vitro* growth in minimal medium [12]. While this defect may be attributable to deficient iron uptake during infection, it is notable that the enterobactin and salmochelin siderophore systems remain functional in this mutant, representing alternative iron uptake systems. A previous analysis also found 15-fold more Cu(II)-Ybt complexes than Fe(III)-Ybt complexes in this infection model [3]. Although *E. coli* have long been regarded to lack a copper import system, these data raise the question of whether UPEC import copper(II)-Ybt as a nutritional source of copper during infections.

In this study, we used direct mass spectrometric quantification to determine whether UPEC obtain copper from Cu(II)-Ybt. Using quantitative mass spectrometry, we found that UPEC can quantitatively convert copper to Cu(II)-Ybt during growth in low copper conditions. In combination with ^{64}Cu radiolabeling, we then found that the FyuA-YbtPQ import system imports Cu(II)-Ybt and removes the bound copper. The results support YbtPQ-facilitated, non-destructive metal-Ybt complex dissociation followed by recycling of liberated, metal-

free Ybt. Copper liberated by this import system supported the copper-dependent enzymatic activity of *E. coli* amine oxidase, a classic cuproenzyme that produces a highly specific product. Together, these results support a role for Ybt in a metallophore system that minimizes copper toxicity while retaining nutritional access to this important biometal, a strategy termed nutritional passivation.

Results

Cu(II)-Ybt forms during low copper UPEC growth

In high copper environments, Ybt protects UPEC by sequestering copper in a stable Cu(II)-Ybt complex [3]. To determine whether UPEC similarly secrete Ybt and sequester copper in low (non-toxic) copper environments, we used LC-MS/MS to quantify Ybt in 20 hour M63/glycerol minimal medium culture supernatants from the model *E. coli* uropathogen UTI89 (Fig 1). We quantified Cu(II)-Ybt formation during culture and then measured the total copper-binding capacity of secreted Ybt by performing a second Cu(II)-Ybt quantification after adding excess $CuSO_4$ (5 mM) to the supernatant. In unsupplemented medium, Ybt copper binding capacity (5.1 μM) substantially exceeded Cu(II)-Ybt (0.6 μM) following 20 hours of UTI89 growth (Fig 1a). This low Cu(II)-Ybt level corresponded to the low copper content of this minimal medium (<4 μM by ICP-MS). When cultures were supplemented with 5 μM $CuSO_4$, Ybt copper binding capacity still exceeded Cu(II)-Ybt concentration (10.1 μM and 5.4 μM, respectively) with no significant impact on final bacterial growth density (Fig 1b). The increase in Cu(II)-Ybt concentration (from 0.6 to 5.4 μM) with copper supplementation was consistent with nearly quantitative copper chelation by Ybt. Metal-free Ybt was readily detectable in both conditions, accounting for the observed excess Cu(II) binding capacity (Fig 1c). Together, these data indicated that UPEC can direct copper speciation toward Cu(II)-Ybt in both low and high copper conditions. This raises the possibility that pathogenic bacteria may benefit from an ability to access copper from Cu(II)-Ybt to support nutritional demands during infection.

UPEC dissociate Cu(II)-Ybt and regenerate Ybt

To determine whether Ybt-bound copper is accessible to *E. coli*, we used quantitative LC-MS/MS to compare cellular interactions between extracellular metal-Ybt complexes and UTI89. The K12 *E. coli* strain MG1655, which lacks the *Yersinia* HPI and does not synthesize Ybt or express known Ybt importers, was used as a control strain [6]. Each bacterial inoculum was washed, resuspended at high density (0.8 OD600 units) in M63 minimal medium, and incubated for 2 hours. To distinguish exogenously supplied Ybt from natively synthesized Ybt, we supplemented the medium with a low concentration (0.1 μM) of stable isotope-labeled Cu(II)-[$^{13}C_6$]Ybt or Fe(III)-[$^{13}C_6$]Ybt.UTI89, but not MG1655, depleted Cu(II)-[$^{13}C_6$]Ybt from the test medium, consistent with FyuA-mediated uptake [13] (Fig 2a). Notably, we also observedUTI89-specific appearance of metal-free [$^{13}C_6$]Ybt in the test medium, consistent with cell-mediated Cu(II)-Ybt dissociation and secretion of the resulting intact, metal-free metallophore (Fig 2b). Substitution of Cu(II)-[$^{13}C_6$]Ybt with the canonical import substrate Fe(III)-[$^{13}C_6$]Ybt yielded analogous results, with UTI89-specific Fe(III)-[$^{13}C_6$]Ybt depletion and generation of metal-free [$^{13}C_6$]Ybt in the test medium (Fig

2c, d). Together, these findings suggest that *E. coli* expressing the *Yersinia* HPI are capable of dissociating both Cu(II)-Ybt and Fe(III)-Ybt complexes.

Cu(II)-Ybt uptake and dissociation require FyuA and YbtPQ

To identify specific determinants of Cu(II)-Ybt and Fe(III)-Ybt import in uropathogenic *E. coli*, we used LC-MS/MS to quantify Ybt in *E. coli* ectopically expressing outer and inner membrane proteins FyuA and YbtPQ. These proteins were expressed in UTI89Δ*ybtA*, a transcriptionally-silenced YbtA-deficient strain incapable of yersiniabactin biosynthesis and Fe(IIII)-Ybt-dependent growth (Supplementary Results, Supplementary Fig 1) [8,21]. In UTI89Δ*ybtA* cultures, exogenously-supplied Cu(II)-Ybt remained extracellular (Fig 3a). UTI89Δ*ybtA* expressing FyuA (UTI89Δ*ybtA* p*fyuA*) depleted Cu(II)-Ybt from the medium and increased cell-associated Cu(II)-Ybt, consistent with outer membrane transport to the periplasm [13]. UTI89Δ*ybtA* co-expressing both FyuA and YbtPQ (UTI89Δ*ybtA* p*fyuA* p*ybtPQ*) depleted Cu(II)-Ybt in both medium and cells while increasing metal-free Ybt in the medium (Fig 3a, b, c). Cultures supplemented with the canonical substrate Fe(III)-Ybt, yielded analogous results (Fig 3d, e, f). Together, these observations indicate that FyuA and Ybt PQ are sufficient to import iron and copper-Ybt complexes in *E. coli*, and YbtPQ is specifically required for complex dissociation to yield metal-free Ybt.

Non-reducible Ga(III)-Ybt complexes are not recycled

Iron extraction from siderophore complexes often involves Fe(III) reduction (to Fe(II), which has significantly lower siderophore binding affinity) in the presence or absence of covalent siderophore modification (through hydrolysis or acetylation)to diminish metal ion affinity [17,22–25]. The *Yersinia* HPI lacks known siderophore hydrolase or reductase genes that would suggest how this process proceeds for yersiniabactin complexes. The appearance of metal-free Ybt following metal-Ybt import (Figs 2, 3) is consistent with reduction-only dissociation without covalent siderophore modification. To assess the role of a purely reductive dissociation pathway, we used Ga(III)-Ybt as a non-reducible chemical probe [13]. Ga(III) and Fe(III) share comparable atomic radii, coordination chemistry, and charge, which allows Ga(III) to substitute for Fe(III) in many siderophore complexes [26,27]. Unlike Fe(III), Ga(III) cannot be reduced to Ga(II) under physiological conditions, making it a non-reducible metal ion probe [28,29]. When Ga(III)-Ybt was substituted for Cu(II)-Ybt and Fe(III)-Ybtin the experimental system described in Fig 3a-f, FyuA expression is again necessary for import and cell-association (Fig 3g) [13]. Unlike Cu(II)-Ybt and Fe(III)-Ybt, Ybt PQ expression neither diminished cell-associated Ga(III)-Ybt nor increased extracellular metal-free Ybt (Fig 3h, i). These findings are consistent with Ga(III)-Ybt as an import substrate that resists cellular dissociation, as predicted for reductive dissociation of Ybt complexes.

Cu(II)-Ybt and Fe(III)-Ybt can be reductively dissociated

To further assess the plausibility of purely reductive Cu(II)-Ybt and Fe(III)-Ybt dissociation, we examined *in vitro* release of Cu(I) from Cu(II)-Ybt and Fe(II) from Fe(III)-Ybt using a previously described *in vitro* system [30]. At pH 7, Cu(II)-Ybt or Fe(III)-Ybt were incubated with ascorbic acid, a reductant with a physiologically accessible reduction potential [31], and a chelator that serves as a model for small molecules or protein side chains that would bind

Cu(I) or Fe(II) following *in vivo* reduction [30]. In these conditions, ascorbic acid was sufficient to release Cu(I) (Fig 4a, b)or Fe(II) (Fig 4c, d) from their corresponding Ybt complexes at neutral pH. These findings support the plausibility of reductive Cu(II)-Ybt and Fe(III)-Ybt dissociation in *E. coli*.

UPEC can use Cu(II)-Ybt as a nutritional copper source

For the Cu(II)-Ybt import and dissociation pathway to be valuable to UPEC, we hypothesized that the copper obtained from Cu(II)-Ybt complexes can be distributed to cellular cuproproteins. To determine whether Ybt-derived copper remains cell-associated in cells expressing the FyuA/YbtPQ system, we added radioactive ^{64}Cu(II)-Ybt to the experimental system described in Fig 3. As expected, FyuA was necessary for cellular ^{64}Cu accumulation (Fig 5a), mirroring Cu(II)-Ybt localization (Fig 3b). Although FyuA/YbtPQ co-expression led to Cu(II)-Ybt dissociation and secretion of metal-free Ybt (Fig 3c), ^{64}Cu remained cell-associated in bacteria co-expressing these proteins. These observations are consistent with cellular retention of copper extracted from Cu(II)-Ybt in UPEC.

To determine if copper extracted from Cu(II)-Ybt is nutritionally useful, we measured the activity of the cuproenzyme *E. coli* copper amine oxidase (ECAO or TynA) from cells given Cu(II)-Ybt as a copper source [32]. TynA is a well-characterized periplasmic enzyme that catalyzes the specific conversion of phenylethylamine to phenylacetaldehyde in a copper-dependent manner (Fig 5b) [33,34]. Because UTI89 lacks native TynA expression (*tynA* is absent in the UTI89 genome), we used UTI89 strains ectopically expressing *tynA* as a highly-specific chemical readout of cuproenzyme activity. To measure TynA activity, we developed a quantitative and specific LC-MS/MS assay to measure phenylacetaldehyde levels in cell lysates that were incubated with phenylethylamine. In an otherwise low copper medium, Cu(II)-Ybt addition (0.2 μM) significantly increased TynA activity in wild type UTI89 p*tynA*, while no significant activity changes were detected in YbtPQ-deficient UTI89Δ*ybtPQ* p*tynA* (Fig 5c). TynA activity could be rescued in UTI89Δ*ybtPQ*p*tynA* by $CuSO_4$ addition (50 μM) to the culture medium (Supplementary Fig 2). Together, these results demonstrate that uropathogenic *E. coli* can direct Cu(II)-Ybt-derived copper to cuproenzymes, consistent with nutritional copper import by the yersiniabactin metallophore system.

Discussion

Despite the presence of well-known (and possibly unknown [35]) copper-dependent enzymes, *E. coli* have long been regarded to lack a copper import system. In this study, we show that uropathogenic *E.coli* can use the yersiniabactin system to acquire copper to support copper-dependent enzyme activity (Fig 6). This functionality may be useful both when copper is scarce or when yersiniabactin has converted otherwise toxic levels of copper to Cu(II)-Ybt. The ability to access multiple bound metals may be a necessary accommodation to broad spectrum microbial metallophore systems in general.

Copper toxicity may be particularly relevant to phagolysosomal compartments and other restricted spaces where reactive oxygen species are abundant [36]. By sequestering copper in complexes and catalyzing superoxide dismutation, Ybt can protect pathogenic

Enterobacteriaceae during infections [3,4]. Directing copper speciation toward Ybt complexes, however, has the potential to paradoxically starve the bacterium of this essential metal. In this context, copper deficiency may arise in local environments where there is a molar excess of Ybt over copper. By importing Cu(II)-Ybt and removing its bound copper in a controlled manner, UPEC retain nutritional access to this metal. Analogous, co-existing virulence-associated countermeasures to both copper excess and scarcity have been shown in the fungal pathogens *Cryptococcus neoformans* and *Candida albicans*, where they affect different stages of infection [37–39]. We suggest the term nutritional passivation for the biological strategy of minimizing metal ion toxicity through chelation while preserving nutritional access to the metal. In contrast with the prototypical rationale of acquiring poorly-accessible iron, which appears to be typical of aerobic infection microenvironments [1], metallophores engaged in nutritional passivation remain valuable even when metal ions are abundant.

The similar metabolic fate of Ybt from Fe(III) and Cu(II) complexes suggest shared early import pathways that later diverge to direct each metal ion toits respective trafficking pathway. The putative reductase (or reductases) expected to be required for this process remains unclear, as does its localization within the cell and possible interaction with YbtPQ. Although previous studies in bacteria suggest that cuproenzymes derive their copper from cytoplasmic sources [40,41], our current knowledge of bacterial copper trafficking pathways remains incomplete. The presence of a putative ferric siderophore reductase domain on the cytoplasmic face of IrtAB, a *Mycobacterium tuberculosis* YbtPQ homologue, suggests that these proteins import intact metal-siderophore complexes to the cytoplasm [18]. Rather than incorporating a *cis*-acting reductase domain, YbtPQ may instead recruit a *trans*-acting cytoplasmic reductase to facilitate metal extraction from Ybt complexes. Alternatively, YbtPQ may facilitate periplasmic metal-Ybt dissociation by exporting cytoplasmic reducing equivalents. Although strains lacking YbtPQ are not deficient for Ybt secretion, the possibility also remains that YbtPQ encodes a Ybt export function that is functionally redundant with other *E. coli* export proteins [12,21]. More detailed studies of YbtPQ will be necessary to discern the specific mechanisms by which YbtP and YbtQ function and interact with copper trafficking pathways.

Nutritional demands for copper likely stem from its natural availability and distinctive redox properties, which are used by numerous microbial enzymes to catalyze oxidative reactions. These biochemical reactions would be expected to be operative in the aerobic extracellular niche characteristic of the chronic mouse cystitis model where *ybtPQ*-deficient mutants are markedly disadvantaged [12,42]. To date, copper demand in *E. coli* is tied to the aerobic metabolism-related enzymes Cu, Zn-superoxide dismutase, cytochrome bo oxidase, multi-copper oxidase and amine oxidase [33,43–45]. Of these, bacterial Cu, Zn-superoxide dismutase has been noted to play a particularly important role in bacterial virulence [46]. A recent survey suggests that many other microbial metalloenzymes have yet to be discovered [35]. Further study is necessary to identify influential cuproenzymes that contribute to virulence during UTI and other infections caused by Ybt-producing bacteria.

In disease-associated microenvironments, bacterial pathogens place a premium on biosynthetic efficiency to limit metabolic demands. The yersiniabactin system, like several

other bacterial siderophore systems, mitigates its biosynthetic costs by nondestructive dissociation and recycling following metal uptake [47–49]. By enabling each Ybt molecule to participate in multiple rounds of metal import, UPEC can divert metabolic energy and building blocks to other important cellular functions, while maintaining Ybt concentrations in the bacterial population [50]. This is in contrast to the genetically conserved enterobactin system in UPEC, which requires both covalent siderophore modification and reduction for efficient iron release [17,19]. As a metallophore engaged in nutritional passivation, Ybt recycling may serve as an efficient and rapid response in host microenvironments of varying metal ion composition.

Online Methods

Bacterial strains, plasmids and culture conditions

Uropathogenic *E. coli* isolate UTI89 and the non-uropathogenic K-12 *E. coli* isolate MG1655 were used in this study [51,52]. Strains were grown in LB agar (Becton, Dickson and Company), LB broth (Becton, Dickson and Company) or M63 minimal salts medium [53] with antibiotics as appropriate. Ampicillin (100μg ml^{-1}, Goldbio) and/or chloramphenicol (25μg ml^{-1}, Goldbio) were used for plasmid selection. Arabinose (0.2% v/v, Sigma) and IPTG (1mM, Goldbio) were used for respective plasmid inductions. UTI89 mutant strains used in this study are listed in Supplementary Table 1. In-frame deletions in UTI89 were made using the standard red recombinase method, using pKD4 or pKD13 as a template, as previously described [54,55]. Antibiotic resistance insertions were removed by transforming the strains with pCP20 expressing the FLP recombinase. Plasmids were made using the pTrc99a vector (p*fyuA* and p*tynA*) or a modified pBAD33 vector (p*ybtPQ*), and genes were cloned using standard PCR and recombination techniques. *tynA* was cloned from the MG1655 genome.

Yersiniabactin preparation

Ybt was generated from UTI89Δ*entB* grown in M63 minimal salts medium supplemented with 0.2% glycerol (v/v) and 10mg ml^{-1} niacin (Sigma) as previously described [53]. [$^{13}C_6$]Ybt with a ^{13}C-substituted phenolic ring was produced from UTI89Δ*entB* Δ*ybtS* grown in M63 minimal salts medium supplemented with 0.2% glycerol (v/v), $^{13}C_6$-labeled salicylic acid and 10mg ml^{-1} niacin (Sigma).[$^{13}C_{21}$]Ybt was produced by UTI89Δ*fur* in media supplemented with [$^{13}C_3$]glycerol as previously described [53]. Metal-Ybt complexes were produced by adding iron(III) chloride, copper(II) sulfide or gallium(III) nitrate (Sigma) to Ybt. Metal-Ybt was applied to a methanol conditioned C18 silica column (Sigma) and eluted with 80% methanol as previously described [56]. Eluates were concentrated by lyophilization. Dried samples were resuspended in deionized water and purified through high-performance liquid chromatography (HPLC) using a C18 silica column (Whatman Partisil). Metal-Ybt containing fractions were collected, dried down using a lyophilizer and resuspended in deionized water. Metal-Ybt concentrations were determined using previously described extinction coefficients [56].

Fe(III)-Ybt dependent growth

Starter cultures grown overnight in M63 medium were used to inoculate a M63 culture with 2 mM EDDHA (Complete Green Company) at a common starting OD_{600}. 1 μM HPLC-

purified Fe(III)-Ybt was added to cultures followed by an 18 hour incubation at 37 °C with shaking, as previously described [56]. Bacterial growth was monitored using OD_{600}. Experiments were performed in three biological replicates.

Liquid chromatography-mass spectrometry (LC-MS)

LC-MS analyses were conducted using a Shimadzu UFLC-equipped AB-Sciex 4000 QTrap operated in positive ion mode using a Turbo V ESI ion source and a Thermo LCQ Deca as previously described [53]. The samples were injected onto a Fused-core phenylhexyl column (Ascentis Express, Supelco) with a flow rate of 0.4ml min^{-1} and the following solvents: solvent A (0.1% (v/v) formic acid) and solvent B (90% (v/v) acetonitrile in 0.1% formic acid (v/v)). The ion spray voltage was set to 5kV and the heater temperature was 500°C. The declustering potential, nebulizer gas (G1), auxiliary gas (G2) and collision energy were set at 110V, 40V, 35V and 35V, respectively. Metal-Ybt quantification was carried out by LC-MS/MS in multiple reaction monitoring mode using known collision-induced dissociation fragmentations and Cu(II)-[$^{13}C_{21}$]Ybt or Fe(III)-[$^{13}C_{21}$]Ybt internal standards, and calculated as a ratio of metal-Ybt peak area over internal standard peak area as previously described [56].

Inductively coupled plasma-mass spectrometry (ICP-MS)

Copper concentrations in M63 minimal media were conducted using high resolution ICP-MS (Agilent 7500ce ICP-MS) as done previously [56]. Samples in M63 medium were diluted 50-fold using 2% nitric acid solution to reduce salt concentrations to levels compatible with the ICP-MS instrument. The limit of detection of copper was measured to be 5ug/L in the diluted M63 medium (4 μM in undiluted M63 medium). Machine was calibrated using Environmental calibration standard (Agilent) and PerkinElmer Pure Plus ICP-MS standard (PerkinElmer).

Ybt production in culture

Wild type UTI89 was inoculated in M63 minimal salts medium supplemented with 0 or 5 μM $CuSO_4$. Cultures were normalized for common starting OD600 of 0.001 and grown for 20 hours at 37 °C while shaking. An aliquot of each culture was serially diluted in phosphate-buffered saline (PBS) and plated onto LB agar for CFU determination. Remaining cultures were pelleted and the supernatant was collected for Ybt determination. To measure Cu(II)-Ybt levels, Cu(II)-[$^{13}C_{21}$]Ybt was added to an aliquot of the supernatant before application to a conditioned C18 silica column. To measure total Ybt, a separate aliquot of the clarified supernatant was incubated with excess $CuSO_4$ (5 mM) for 1 hr at room temperature before addition of Cu(II)-[$^{13}C_{21}$]Ybt and application to the C18 column. Experiments were performed in three biological replicates.

Cell-associated metal-Ybt

Strains were grown overnight in M63 minimal salts medium supplemented with 0.2% glycerol (v/v) and 10mg ml^{-1} niacin (Sigma) as previously described [53]. Strains were resuspended to a starting OD600 of 0.8 in fresh M63 with supplements described above. HPLC-purified 0.1μM metal-Ybt was added to cultures followed by a 2 hour incubation at

37 degrees while shaking. Bacteria were pelleted at 7500×g for 10 minutes (Eppendorf) and washed with PBS (Sigma). Fe(III)-[$^{13}C_{21}$]Ybt internal standard was added to the collected supernatant and applied to a conditioned C18 silica column. Bacteria were resuspended in 100% ethanol (Sigma) and pelleted at 20,000 g for 10 minutes. Supernatant was collected and dried for 3 hours using a vacuum concentrator. Samples were resuspended in ultrapure water and applied to a conditioned C18 silica column with added Fe(III)-[$^{13}C_{21}$]Ybt internal standard. Experiments were conducted in three biological replicates.

Fe(III)-Ybt and Cu(II)-Ybt reduction

To investigate Ybt complex reduction, we adapted a previously described *in vitro* system [57]. Fe(III)-Ybt (5 μM), bathophenanthrolinedisulfonic acid disodium salt hydrate (BPDS, 2.5 mM, Sigma), and L-ascorbic acid (50 mM, Sigma) were incubated in phosphate buffer (pH 7, Sigma) for 2 hours at room temperature in a 96 well plate. Fe(II)-BPDS complex formation was measured spectrophotometrically (λ_{max} = 533nm) and Ybt levels were quantified relative to Fe(III)-Ybt with LC-MS/MS [56,57]. For Cu(II)-Ybt reduction bathocuproinedisulfonate (BCP, 2.5 mM, Sigma) was substituted for BPDS. Cu(I)-BCP complex formation was measured spectrophotometrically (λ_{max} = 484 nm) and metal-free Ybt levels were quantified relative to Cu(II)-Ybt with LC-MS/MS [53,56]. Experiments were done in three biological replicates.

^{64}Cu(II)-Ybt Radiolabeling

^{64}Cu ($t_{1/2}$= 12.7 h, β^+=17%, β^-=39%, EC=43%, E_{max}=0.656 MeV) was produced by a (p,n) reaction on enriched ^{64}Ni on a CS-15 biomedical cyclotron (Cyclotron Corporation, Berkeley, CA) at Mallinckrodt Institute of Radiology, Washington University School of Medicine and purified on an automated system using standard procedures [58,59]. A stock solution of ^{64}Cu in 0.05 M HCl was diluted in 0.1 M ammonium acetate (NH_4OAc) buffer solution (pH 7) for radiolabeling purposes. A typical reaction involves using 74 – 111 MBq (2 -3 mCi) of ^{64}Cu added to 20 μL of Ybt (5 nanomoles) and 0.1 M NH_4OAc buffer to bring the reaction volume to 100 μL. The reaction mixture was incubated on a mixer with 800 rpm agitation at 37 °C for 1 hour. Labeling efficiency and radiochemical purity were determined using radio-HPLC (Agilent 1200 system with a Flow-RAM radio-HPLC detector) on a C18 column (Kinetex, Phenomenex). The mobile phase consisted of water (A) and acetonitrile (B) with a gradient of 0 – 100 % B over 10 min using a flow rate of 1 mL/min. The retention time of ^{64}Cu(II)-Ybt was 6.1 min and a radiochemical yield of greater than 99% was achieved and used without further purification.

Cell-associated ^{64}Cu(II)-Ybt

Strains were grown overnight and diluted to an OD600 of 0.8 in M63 minimal medium as described above. HPLC-purified 0.1μM Cu(II)-Ybt and 185,000 counts of ^{64}Cu(II)-Ybt (0.925 μCi) were added to strains and grown for 2 hours while shaking. Bacteria were pelleted at 7500 g for 10 minutes (Eppendorf) and washed with 1× PBS (Sigma) multiple times. Cell-associated ^{64}Cu levels were measured from pelleted bacteria using a gamma counter (Packard II, Perkin Elmer). Experiments were conducted with three biological replicates.

TynA activity quantification

Strains were grown overnight and diluted to an OD600 of 0.8 as described above. For the $CuSO_4$ control, both $CuSO_4$ (50 μM) and $FeCl_3$ (100 μM) were added to the overnight culture. After dilution, HPLC-purified Cu(II)-Ybt (0.2 μM) or $CuSO_4$ (50 μM) plus $FeCl_3$ (100 μM) were added to strains followed by an hour incubation at 37 degrees while shaking. Bacteria were pelleted at 7500 g for 10 minutes (Eppendorf) and washed twice with 1× PBS (Sigma). Bacteria were resuspended in lysis buffer (100 mM sodium phosphate pH 7.0, 2.5 mM magnesium sulfate) with 1 mg/mL lysozyme, DNAse, 100 μM phenylmethylsulfonyl fluoride, and an EDTA-free protease inhibitor tablet (SigmaFast Protease Inhibitor Cocktail Tablet), and lysed by 3 freeze/thaw cycles. The lysate was spun at 20,817 g for 10 minutes at 4 °C. Phenylethylamine (1 mM, Sigma) was added to the clarified lysate and the reaction was incubated for 1 hour at room temperature. The reaction was quenched using lysis buffer with 5% formic acid and 100 μM internal standard (3-fluorophenylacetaldehyde, F-PAA, Sigma) and applied to a conditioned C18 silica column (50 mg, UCT). The column was washed using lysis buffer with 5% formic acid, and eluted in 100% methanol with 5% formic acid. The phenylacetaldehyde product and F-PAA internal standard were derivatized by incubation with semicarbazide (5 mM, Sigma) at 40 °C for 2 hours[60]. The derivatized phenylacetaldehyde (dPAA) product was measured by LC-MS/MS in multiple reaction monitoring mode using known collision-induced dissociation fragmentations. TynA activity was calculated as a ratio of dPAA peak area over dF-PAA peak area and normalized by the final OD600 of each sample. Experiments using Cu(II)-Ybt were conducted in three biological replicates while $CuSO_4$ control experiments were conducted in duplicates.

Statistical analyses

Statistics and graphs were generated using GraphPad Prism 5 (GraphPad software). Unpaired Student's *t*-test (two-tailed) was used to compare between strains.

Data Availability

All data supporting the findings of this study are available within the paper and its supplementary information files are available from the corresponding author on reasonable request.

Supplementary Material

Refer to Web version on PubMed Central for supplementary material.

Acknowledgments

J.P.H. holds a Career Award for Medical Scientists from the Burroughs Wellcome Fund and acknowledges National Institute of Diabetes and Digestive and Kidney Diseases grants R01DK099534 and P50DK064540. ICP-MS was supported by the Nano Research Facility at Washington University in St. Louis. The funders had no role in study design, data collection and interpretation, or the decision to submit the work for publication. We thank Zongsen Zou, Dr. Jennifer Walker, Dr. Lloyd Robinson and Stephanie Krieger for technical assistance, and Shannon Ohlemacher for helpful discussion.

References for Main Text

1. Hood MI, Skaar EP. Nutritional immunity: transition metals at the pathogen–host interface. Nat Rev Microbiolgy. 2012; 10:525–537.
2. Chaturvedi KS, Henderson JP. Pathogenic adaptations to host-derived antibacterial copper. Front Cell Infect Microbiol. 2014; 4:3. [PubMed: 24551598]
3. Chaturvedi KS, Hung CS, Crowley JR, Stapleton AE, Henderson JP. The siderophore yersiniabactin binds copper to protect pathogens during infection. Nat Chem Biol. 2012; 8:731–736. [PubMed: 22772152]
4. Chaturvedi KS, et al. Cupric Yersiniabactin Is a Virulence-Associated Superoxide Dismutase Mimic. ACS Chem Biol. 2013; 9:551–561. [PubMed: 24283977]
5. Greenberg SB, Harris D, Giles P, Martin RR, Wallace RJ. Inhibition of Chlamydia trachomatis growth in McCoy, HeLa, and human prostate cells by zinc. Antimicrob Agents Chemother. 1985; 27:953–957. [PubMed: 4026267]
6. Henderson JP, et al. Quantitative Metabolomics Reveals an Epigenetic Blueprint for Iron Acquisition in Uropathogenic Escherichia coli. PLOS Pathog. 2009; 5:e1000305. [PubMed: 19229321]
7. Perry RD, Balbo PB, Jones HA, Fetherston JD, DeMoll E. Yersiniabactin from Yersinia pestis: biochemical characterization of the siderophore and its role in iron transport and regulation. Microbiology. 1999; 145:1181–1190. [PubMed: 10376834]
8. Fetherston JD, Bearden SW, Perry RD. YbtA, an AraC-type regulator of the Yersinia pestispesticin/yersiniabactin receptor. Mol Microbiol. 1996; 22:315–25. [PubMed: 8930916]
9. Fetherston JD, Bertolino VJ, Perry RD. YbtP and YbtQ: two ABC transporters required for iron uptake in Yersinia pestis. Mol Microbiol. 1999; 32:289–99. [PubMed: 10231486]
10. Reigstad CS, Hultgren SJ, Gordon JI. Functional genomic studies of uropathogenic Escherichia coli and host urothelial cells when intracellular bacterial communities are assembled. J Biol Chem. 2007; 282:21259–67. [PubMed: 17504765]
11. Brumbaugh AR, et al. Blocking Yersiniabactin Import Attenuates Extraintestinal Pathogenic Escherichia coli in Cystitis and Pyelonephritis and Represents a Novel Target To Prevent Urinary Tract Infection. Infect Immun. 2015; 83:1443–1450. [PubMed: 25624354]
12. Koh EI, Hung CS, Henderson JP. The Yersiniabactin-Associated ATP Binding Cassette Proteins YbtP and YbtQ Enhance Escherichia coli Fitness during High-Titer Cystitis. Infect Immun. 2016; 84:1312–1319. [PubMed: 26883590]
13. Koh EI, et al. Metal selectivity by the virulence-associated yersiniabactin metallophore system. Metallomics. 2015; 7:1011–1022. [PubMed: 25824627]
14. Lukacik P, et al. Structural engineering of a phage lysin that targets Gram-negative pathogens. PNAS. 2012; 109:9857–9862. [PubMed: 22679291]
15. Rodriguez GM, Smith I. Identification of an ABC transporter required for iron acquisition and virulence in Mycobacterium tuberculosis. J Bacteriol. 2006; 188:424–30. [PubMed: 16385031]
16. Perry RD, Fetherston JD. Yersiniabactin iron uptake: mechanisms and role in Yersinia pestis pathogenesis. Microbes Infect Inst Pasteur. 2011; 13:808–17.
17. Miethke M, Hou J, Marahiel MA. The siderophore-interacting protein YqjH acts as a ferric reductase in different iron assimilation pathways of Escherichia coli. Biochemistry (Mosc). 2011; 50:10951–64.
18. Ryndak MB, Wang S, Smith I, Rodriguez GM. The Mycobacterium tuberculosis High-Affinity Iron Importer, IrtA, Contains an FAD-Binding Domain. J Bacteriol. 2010; 192:861–869. [PubMed: 19948799]
19. Lin H, Fischbach MA, Liu DR, Walsh CT. In Vitro Characterization of Salmochelin and EnterobactinTrilactone Hydrolases IroD, IroE, and Fes. J Am Chem Soc. 2005; 127:11075–11084. [PubMed: 16076215]
20. Koh EI, Henderson JP. Microbial Copper-binding Siderophores at the Host-Pathogen Interface. J Biol Chem. 2015; 290:18967–18974. [PubMed: 26055720]

21. Lv H, Henderson JP. Yersinia High Pathogenicity Island Genes Modify the Escherichia coli Primary Metabolome Independently of Siderophore Production. J Proteome Res. 2011; 10:5547–5554. [PubMed: 22035238]
22. Cooper SR, McArdle JV, Raymond KN. Siderophore electrochemistry: relation to intracellular iron release mechanism. Proc Natl Acad Sci U S A. 1978; 75:3551–4. [PubMed: 151277]
23. Raymond KN, Dertz EA, Kim SS. Enterobactin : an archetype for microbial iron transport. Proc Natl Acad Sci U S A. 2003; 100:3584–8. [PubMed: 12655062]
24. Harrington JM, Crumbliss AL. The redox hypothesis in siderophore-mediated iron uptake. Biometals. 2009; 22:679–689. [PubMed: 19357971]
25. Hannauer M, Barda Y, Mislin GLA, Shanzer A, Schalk IJ. The Ferrichrome Uptake Pathway in Pseudomonas aeruginosa Involves an Iron Release Mechanism with Acylation of the Siderophore and Recycling of the Modified Desferrichrome. J Bacteriol. 2010; 192:1212–1220. [PubMed: 20047910]
26. Olakanmi O, Britigan BE, Schlesinger LS. Gallium Disrupts Iron Metabolism of Mycobacteria Residing within Human Macrophages. Infect Immun. 2000; 68:5619–5627. [PubMed: 10992462]
27. Hubbard JAM, Lewandowska KB, Hughes MN, Poole RK. Effects of iron-limitation of Escherichia coli on growth, the respiratory chains and gallium uptake. Arch Microbiol. 1986; 146:80–86. [PubMed: 3545122]
28. Bernstein LR. Mechanisms of Therapeutic Activity for Gallium. Pharmacol Rev. 1998; 50:665–682. [PubMed: 9860806]
29. Emery T. Exchange of iron by gallium in siderophores. Biochemistry (Mosc). 1986; 25:4629–4633.
30. Mies KA, Wirgau JI, Crumbliss AL. Ternary complex formation facilitates a redox mechanism for iron release from a siderophore. Biometals Int J Role Met Ions Biol Biochem Med. 2006; 19:115–26.
31. Creutz C. Complexities of ascorbate as a reducing agent. Inorg Chem. 1981; 20:4449–4452.
32. Klinman JP. The multi-functional topa-quinone copper amine oxidases. Biochim Biophys Acta BBA - Proteins Proteomics. 2003; 1647:131–137. [PubMed: 12686122]
33. Parsons M, et al. Crystal structure of a quinoenzyme: copper amine oxidase of Escherichia coli at 2 å resolution. Structure. 1995; 3:1171–1184. [PubMed: 8591028]
34. Smith MA, et al. Exploring the Roles of the Metal Ions in Escherichia coli Copper Amine Oxidase. Biochemistry (Mosc). 2010; 49:1268–1280.
35. Cvetkovic A, et al. Microbial metalloproteomes are largely uncharacterized. Nature. 2010; 466:779–82. [PubMed: 20639861]
36. White C, Lee J, Kambe T, Fritsche K, Petris MJ. A role for the ATP7A copper-transporting ATPase in macrophage bactericidal activity. J Biol Chem. 2009; 284:33949–56. [PubMed: 19808669]
37. Sun TS, et al. Reciprocal functions of Cryptococcus neoformans copper homeostasis machinery during pulmonary infection and meningoencephalitis. Nat Commun. 2014; 5:5550. [PubMed: 25417972]
38. Ding C, et al. The Cu regulon of the human fungal pathogen Cryptococcus neoformans H99: Cuf1 activates distinct genes in response to both Cu excess and deficiency. Mol Microbiol. 2011; 81:1560–1576. [PubMed: 21819456]
39. Li CX, et al. Candida albicans adapts to host copper during infection by swapping metal cofactors for superoxide dismutase. Proc Natl Acad Sci. 2015; 112:E5336–E5342. [PubMed: 26351691]
40. Osman D, et al. The copper supply pathway to a Salmonella Cu, Zn-superoxide dismutase (SodCII) involves P(1B)-type ATPase copper efflux and periplasmic CueP. Mol Microbiol. 2013; 87:466–77. [PubMed: 23171030]
41. Gold B, et al. Identification of a copper-binding metallothionein in pathogenic mycobacteria. Nat Chem Biol. 2008; 4:609–616. [PubMed: 18724363]
42. Hannan TJ, Mysorekar IU, Hung CS, Isaacson-Schmid ML, Hultgren SJ. Early Severe Inflammatory Responses to Uropathogenic E. coli Predispose to Chronic and Recurrent Urinary Tract Infection. PLOS Pathog. 2010; 6:e1001042. [PubMed: 20811584]

43. Imlay KR, Imlay JA. Cloning and analysis of sodC, encoding the copper-zinc superoxide dismutase of Escherichia coli. J Bacteriol. 1996; 178:2564–2571. [PubMed: 8626323]
44. van der Oost J, et al. Restoration of a lost metal-binding site: construction of two different copper sites into a subunit of the E. coli cytochrome o quinol oxidase complex. EMBO J. 1992; 11:3209–3217. [PubMed: 1324168]
45. Roberts SA, et al. A Labile Regulatory Copper Ion Lies Near the T1 Copper Site in the Multicopper Oxidase CueO. J Biol Chem. 2003; 278:31958–31963. [PubMed: 12794077]
46. Kim B, Richards SM, Gunn JS, Slauch JM. Protecting against antimicrobial effectors in the phagosome allows SodCII to contribute to virulence in Salmonella enterica serovar Typhimurium. J Bacteriol. 2010; 192:2140–9. [PubMed: 20154132]
47. Hibbing ME, Fuqua C, Parsek MR, Peterson SB. Bacterial competition: surviving and thriving in the microbial jungle. Nat Rev Microbiol. 2010; 8:15–25. [PubMed: 19946288]
48. Jones CM, et al. Self-poisoning of Mycobacterium tuberculosis by interrupting siderophore recycling. Proc Natl Acad Sci. 2014; 111:1945–1950. [PubMed: 24497493]
49. Imperi F, Tiburzi F, Visca P. Molecular basis of pyoverdine siderophore recycling in Pseudomonas aeruginosa. PNAS. 2009; 106:20440–20445. [PubMed: 19906986]
50. Lv H, Hung CS, Henderson JP. Metabolomic analysis of siderophore cheater mutants reveals metabolic costs of expression in uropathogenic Escherichia coli. J Proteome Res. 2014; 13:1397–404. [PubMed: 24476533]

Methods-Only Reference

51. Chen SL, et al. Identification of genes subject to positive selection in uropathogenic strains of Escherichia coli: a comparative genomics approach. Proc Natl Acad Sci U S A. 2006; 103:5977–82. [PubMed: 16585510]
52. Blattner FR, et al. The Complete Genome Sequence of Escherichia coli K-12. Science. 1997; 277:1453–1462. [PubMed: 9278503]
53. Chaturvedi KS, Hung CS, Crowley JR, Stapleton AE, Henderson JP. The siderophore yersiniabactin binds copper to protect pathogens during infection. Nat Chem Biol. 2012; 8:731–736. [PubMed: 22772152]
54. Lv H, Henderson JP. Yersinia High Pathogenicity Island Genes Modify the Escherichia coli Primary Metabolome Independently of Siderophore Production. J Proteome Res. 2011; 10:5547–5554. [PubMed: 22035238]
55. Datsenko KA, Wanner BL. One-step inactivation of chromosomal genes in Escherichia coli K-12 using PCR products. PNAS. 2000; 97:6640–6645. [PubMed: 10829079]
56. Koh EI, et al. Metal selectivity by the virulence-associated yersiniabactin metallophore system. Metallomics. 2015; 7:1011–1022. [PubMed: 25824627]
57. Mies KA, Wirgau JI, Crumbliss AL. Ternary complex formation facilitates a redox mechanism for iron release from a siderophore. Biometals Int J Role Met Ions Biol Biochem Med. 2006; 19:115–26.
58. McCarthy DW, et al. Efficient production of high specific activity 64Cu using a biomedical cyclotron. Nucl Med Biol. 1997; 24:35–43. [PubMed: 9080473]
59. Kume M, et al. A semi-automated system for the routine production of copper-64. Appl Radiat Isot. 2012; 70:1803–1806. [PubMed: 22516717]
60. Berdyshev EV, et al. Characterization of sphingosine-1-phosphate lyase activity by electrospray ionization-liquid chromatography/tandem mass spectrometry quantitation of (2E)-hexadecenal. Anal Biochem. 2011; 408:12–18. [PubMed: 20804717]

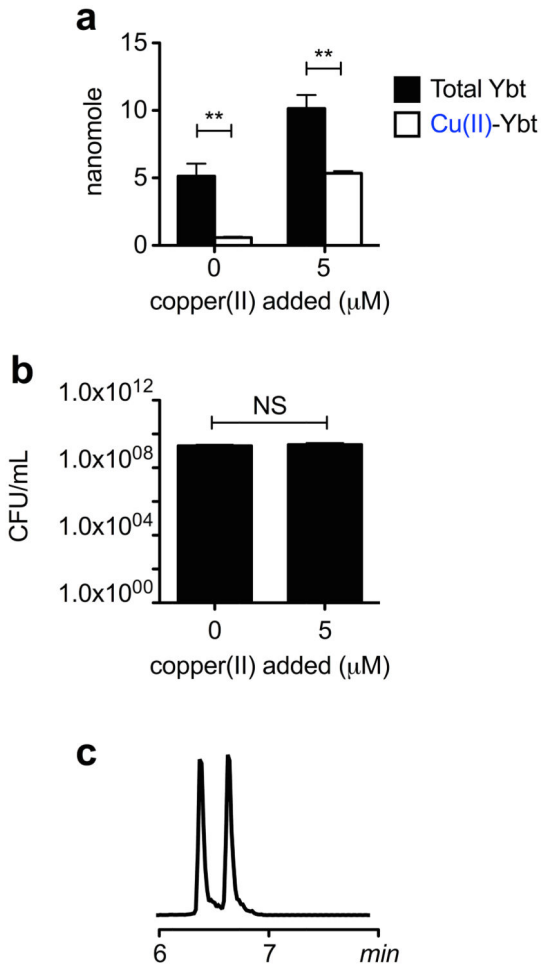

Figure 1.

Cu(II)-Ybt formation during low copper UPEC growth. (a) In cultures of UTI89 grown in M63 minimal medium (20 hours), the total copper-binding capacity of secreted Ybt (total Ybt) exceeded available copper. Following 5 μM $CuSO_4$ addition to the culture medium, excess copper-binding capacity was sustained, with a proportional increase in Cu(II)-Ybt. (b) $CuSO_4$ addition did not significantly affect UTI89 growth density.(c) Metal-free Ybt was detectable in unsupplemented medium. LC-MS/MS chromatogram (*m/z* 482→295) of culture supernatant showed the two isomer peaks of metal-free Ybt. Results are shown as mean ± s.d., n=3, $^{**}P \leq 0.01$ based on a *t*-test; NS, non-significant; CFU, colony forming units.

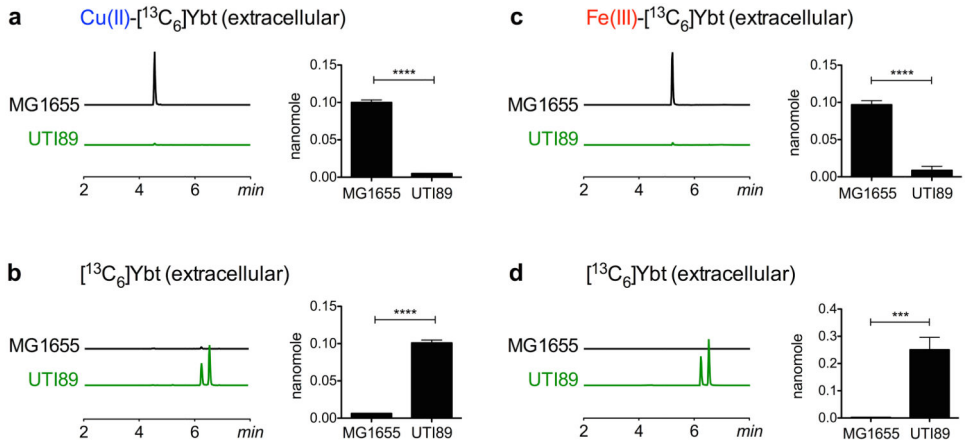

Figure 2.

UPEC convert Cu(II)-Ybt and Fe(III)-Ybt to metal-free Ybt. High density cultures of model uropathogen UTI89 and K12 strain MG1655 were supplemented with 0.1 μM Cu(II)-[$^{13}C_6$]Ybt or Fe(III)-[$^{13}C_6$]Ybt in M63 minimal medium for 2 hours. The model uropathogen UTI89, but not the K12 strain MG1655, dissociated Cu(II)-Ybt and Fe(III)-Ybt complexes, regenerating metal-free Ybt. Representative LC-MS/MS chromatograms of extracellular Cu(II)-[$^{13}C_6$]Ybt (a, *left*) or metal-free [$^{13}C_6$]Ybt (shown as two isomer peaks) (b, *left*) from UTI89 and MG1655 cultures. Each chromatogram was scaled to its internal standard peak height. LC-MS/MS quantification revealed significantly decreased extracellular Cu(II)-[$^{13}C_6$]Ybt (a, *right*) and increased extracellular metal-free [$^{13}C_6$]Ybt (b, *right*) in UTI89. Representative LC-MS/MS chromatograms of extracellular Fe(III)-[$^{13}C_6$]Ybt (c, *left*) or metal-free [$^{13}C_6$]Ybt (shown as two isomer peaks) (d, *left*) from UTI89 and MG1655 cultures. LC-MS/MS quantification revealed significantly decreased extracellular Fe(III)-[$^{13}C_6$]Ybt (c, *right*) and increased extracellular metal-free [$^{13}C_6$]Ybt (d, *right*) in UTI89. Results are shown as mean ±s.d.; n=3; ***P < 0.001, ****P < 0.0001 based on a t-test.

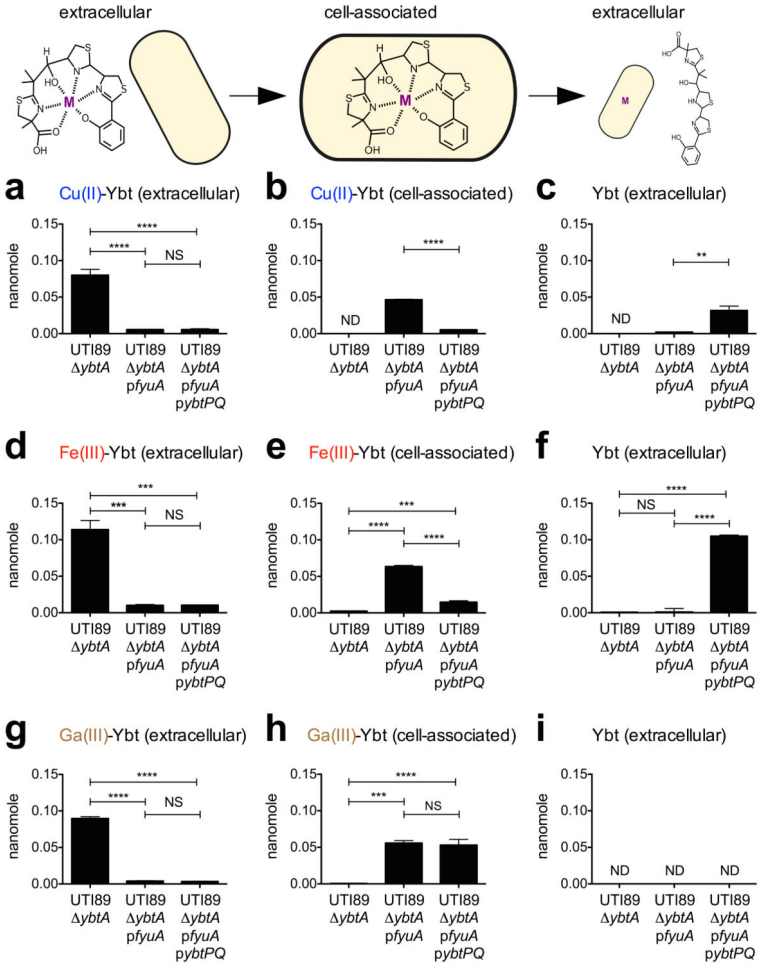

Figure 3.

Requirements for Ybt complex uptake and dissociation. Cu(II)-, Fe(III)-and Ga(III)-Ybt, and metal-free Ybt were quantified in UTI89 cultures supplemented with respective metal-Ybt complex (0.1 μM).(a, d, g) Extracellular metal-Ybt complexes remained extracellular in UTI89Δ*ybtA,* a strain lacking HPI expression. (b, e, h) YbtPQ expression (UTI89Δ*ybtA* p*fyuA* p*ybtPQ* compared to UTI89Δ*ybtA* p*fyuA*) significantly diminished cell-associated levels of Fe(III)-Ybt and Cu(II)-Ybt but not redox inactive Ga(III)-Ybt.(c, f, i) YbtPQ expression caused a corresponding increase in extracellular, metal-free Ybt accumulation in cultures supplemented with Cu(II)- and Fe(III)-Ybt but not Ga(III)-Ybt. Results are shown as mean ± s.d.; n=3; ****P < 0.0001 based on a t-test, NS = non-significant, ND = not detected.

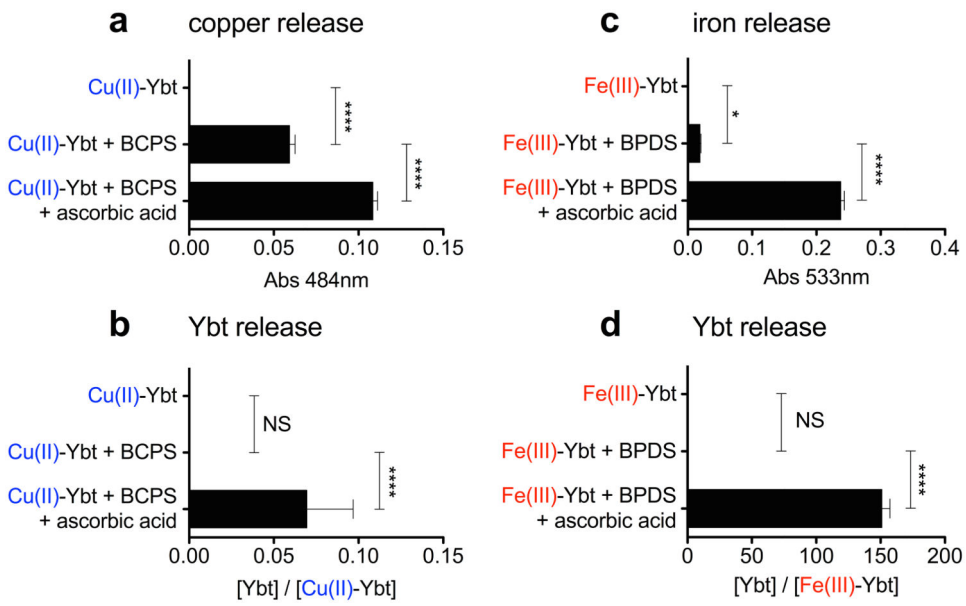

Figure 4.

Reductive dissociation of Cu(II)-Ybt and Fe(III)-Ybt. (a, b) Cu(II)-Ybt (5 μM) and (c, d) Fe(III)-Ybt(5 μM) were incubated with BCPS (bathocuproinedisulfonate, 2.5 mM) orBPDS (bathophenanthrolinedisulfonic acid, 2.5mM) respectively in PBS for 2 hours. In the case for Fe(III)-Ybt, bathophenanthroline (BPDS) was used as the Fe(II) acceptor, while bathocuproinedisulfonate (BCPS) was used as the Cu(I) chelator for Cu(II)-Ybt. Addition of reducing agent (50 mM ascorbic acid) resulted in significantly increased (a) Cu(I) and (c) Fe(II) release, and (b, d) metal-free Ybt. Results are shown as mean ± s.d.; n=3; ****P < 0.0001 based on a t-test, NS = non-significant.

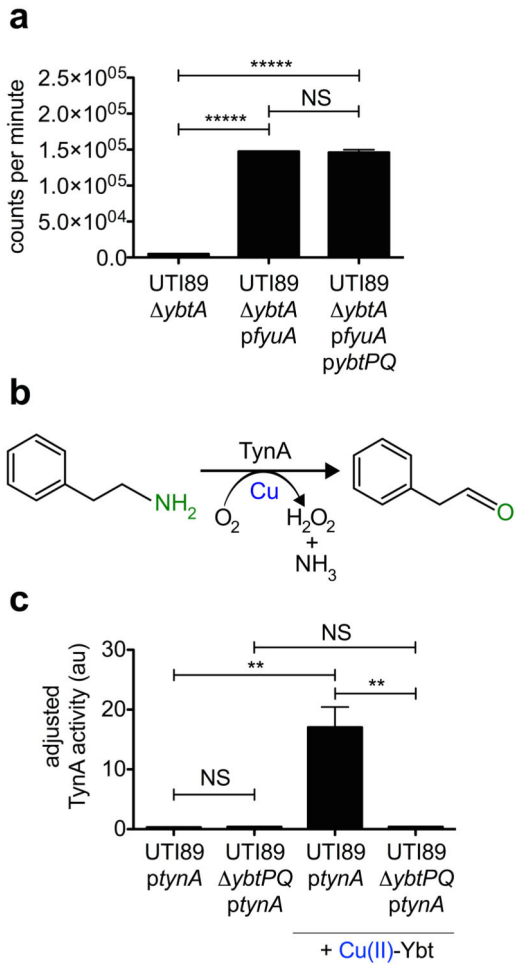

Figure 5.

Cu(II)-Ybt as a nutritional copper source in *E. coli*. (a) Comparable cellular copper accumulation (measured as ^{64}Cu counts per minute) in UTI89Δ*ybtA* p*fyuA* and UTI89Δ*ybtA* p*fyuA* p*ybtPQ* following supplementation with Cu(II)-Ybt (0.1 μM) and ^{64}Cu(II)-Ybt. (b) *E. coli* amine oxidase (TynA) selectively catalyzes phenylethylamine deamination to phenylacetaldehyde, ammonia, and peroxide in a copper-dependent manner. (c) TynA activity in UTI89 p*tynA* grown in M63 minimal medium was dependent upon addition of exogenous Cu(II)-Ybt (0.2μM) and YbtPQ expression. Results are shown as mean ± s.d., n=3, $^{**}P \leq 0.01$, $^{****}P < 0.0001$ based on a *t*-test; NS, non-significant.

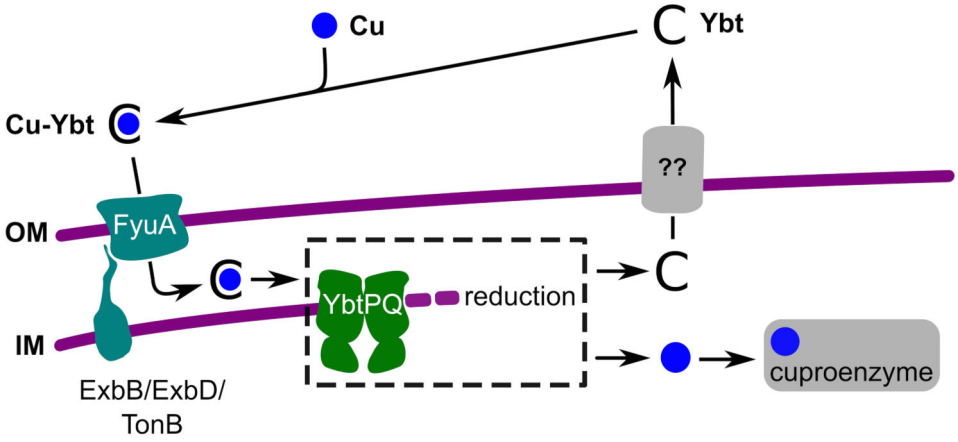

Figure 6.

Model of Cu(II)-Ybt transport, utilization and recycling. Extracellular Ybt interacts with copper to form stable Cu(II)-Ybt complexes. Cu(II)-Ybt import requires the outer membrane receptor FyuA and the inner membrane TonB complex. The ATP-binding cassette transporters YbtP and YbtQ are necessary for Cu(II)-Ybt dissociation and nutritional copper use. YbtPQ activity is unclear and may involve cytoplasmic Cu(II)-Ybt import or periplasmic Cu(II)-Ybt dissociation (black dotted box). Metal-free Ybt released by this process is secreted while copper is directed to cuproenzymes.